SABOT, OBTURATOR AND GAS-IN-LAUNCH TUBE TECHNIQUES FOR HEAT FLUX MODELS IN BALLISTIC RANGES

David W. Bogdanoff[*] and Michael C. Wilder[§]

[*]ERC Inc., NASA Ames Research Center, Moffett Field. CA 94035-1000

[§]NASA Ames Research Center, Moffett Field. CA 94035-1000

Summary: For thermal protection system (heat shield) design for space vehicle entry into earth and other planetary atmospheres, it is essential to know the augmentation of the heat flux due to vehicle surface roughness. At the NASA Ames Hypervelocity Free Flight Aerodynamic Facility (HFFAF) ballistic range, a campaign of heat flux studies on rough models, using infra-red camera techniques, has been initiated. Several phenomena can interfere with obtaining good heat flux data when using this measuring technique. These include leakage of the hot drive gas in the gun barrel through joints in the sabot (model carrier) to create spurious thermal imprints on the model forebody, deposition of sabot material on the model forebody, thereby changing the thermal properties of the model surface and unknown in-barrel heating of the model. This report presents developments in launch techniques to greatly reduce or eliminate these problems. The techniques include the use of obturator cups behind the launch package, enclosed versus open front sabot designs and the use of hydrogen gas in the launch tube. Attention also had to be paid to the problem of the obturator drafting behind the model and impacting the model. Of the techniques presented, the obturator cups and hydrogen in the launch tube were successful when properly implemented.

I. INTRODUCTION

NASA has recently initiated a project to improve Thermal Protection System (TPS) technology and design for outer planet missions, which was motivated by the recommendation of the National Research Council[1]. The approach is to invest in the technology development tasks needed to deliver the capabilities to embark on three new outer planet missions during the coming decade. These missions include a Saturn Atmospheric Probe Mission[2,3], and a Uranus Orbiter and Probe mission[4].To achieve the probe mission goals, thermal protection system (TPS) technologies capable of withstanding extreme environmental entry conditions needs must be sustained and improved to protect the probe's science payload.

This technology development project aims to fill current gaps in testing and design capabilities required to qualify and certify both heritage and alternative TPS materials for Outer Planet exploration, and to support the research and development of new TPS technologies that could enable better science return for the extreme entry environments by lowering the overall probe mass. One sub-task focuses on quantifying the effects of surface roughness on turbulent convective heating. Such effects are of particular importance when ablative TPS materials are required. As the TPS material ablates on entry, a surface roughness characteristic of the material forms. Roughness can significantly increase the surface heating, with the degree of augmentation depending on the roughness size relative to the flow scales at the surface. This heating augmentation is typically mitigated by increasing TPS thickness, which consequently decreases the mission science payload fraction.

Systematic experiments are underway in the NASA Ames Hypervelocity Free Flight Aerodynamic Facility (HFFAF) ballistic range to develop a heating augmentation database in

relevant entry environments. The facility uniquely provides the capability of testing model vehicles in hypersonic flight through controlled, quiescent environments, which allows these tests to be conducted at conditions that match several key parameters of full-scale flight. These parameters include the roughness scale relative to the boundary-layer scale, the smooth-wall turbulent convective heating rates, and in some cases, the free stream Reynolds number.

The technique to measure the heat flux incident on the models in the ballistic range involves measuring the visible and infra-red (3 – 5 microns) emission from the model surface using calibrated cameras. Each camera takes a single frame picture of the model at some point in its flight down the range. Knowing the emissivity of the model surface, the model surface temperatures can be obtained. With the model surface temperature distribution known at several locations down the length of the range, the heat flux histories to the model surface can be calculated using the one-dimensional heat conduction equation. Further details of the technique are given in Ref. 5.

The present paper deals with several effects which can interfere with obtaining high quality heat flux measurements in the ballistic range and details the techniques which were developed to eliminate or minimize these effects. One effect is that the drive gas behind the launch package in the gun barrel can leak through the sabot (model carrier) structure and reach the model forebody and leave thermal imprints which can confound the measurement of range heat fluxes on the forebody. A second effect can occur when parts of the sabot are located upstream of the model. Hot gas from in front of the model can flow through joint gaps in the sabot and deposit sabot material on the model forebody, thereby changing the model's thermal and emissive characteristics in unknown ways. A third effect is the unknown in-barrel heating which occurs when an open barrel is used with an open front sabot. The latter effect can, in principle, be dealt with by the use of a sabot design enclosing the model or by placing a diaphragm at the muzzle and filling the barrel with the test gas at a much lower pressure than in the range or with a higher sound speed gas such as hydrogen. Both techniques are discussed in the following sections.

II. TEST FACILITY AND CAMERAS

Figure 1 shows a top view of the uprange end of the NASA Ames HFFAF ballistic range. The HFFAF is an enclosed, controlled-pressure aeroballistic range with a 22.9 meter-long test section over which 16 evenly spaced spark shadowgraph stations are distributed. Only the first.
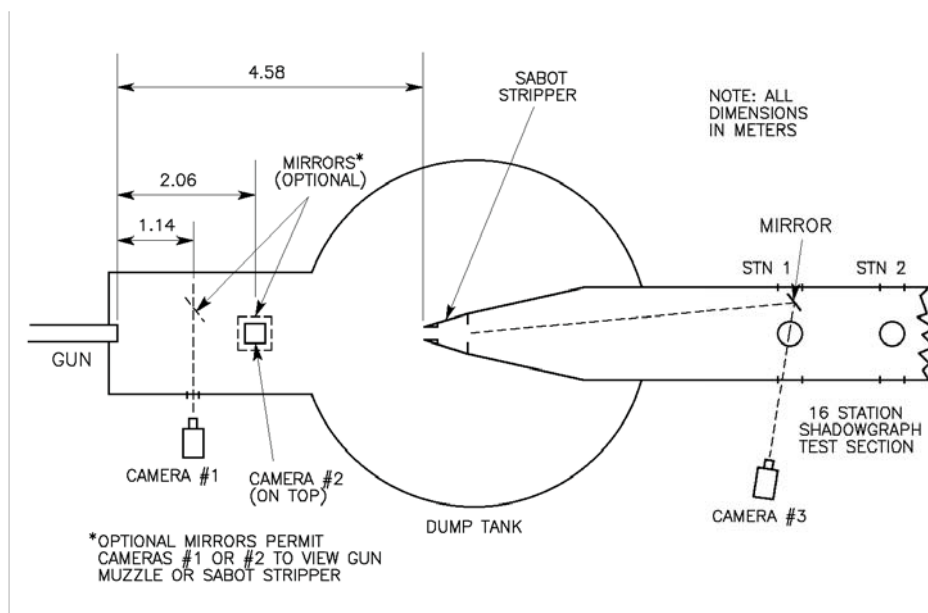
Figure 1. Top view of NASA Ames HFFAF ballistic range showing movie camera set-up.

two shadowgraph stations are shown in Fig. 1. Each station provides orthogonal side- and top-view shadowgraphs from which a projectile's 6 degrees-of-freedom (DOF) trajectory information – 3 position and 3 angle components – can be measured. Elapsed-time data, provided by 16 high-speed digital counters synchronized with the shadowgraphs, allow velocities and angular rates to be obtained from the measured trajectories. The HFFAF has a variety of launchers, which give it the capability to attain projectile velocities from the subsonic to the hypersonic regime. A two stage light gas gun with a launch tube diameter of 3.81 cm was used for the present test campaign. Figure 1 shows the locations of 3 digital movie cameras used to view launch package exit from the muzzle, sabot separation and model flight. At shadowgraph stations 3, 8 and 13, mid-wave infra-red (3 – 5 microns) FLIR/Indigo Phoenix (stations 3 and 8) or FLIR SC8000 (station 13) cameras are used to take 0.5 – 1.0 microsec exposure near head-on photos of the models. Figure 2 shows a representative set-up for the infra-red cameras.
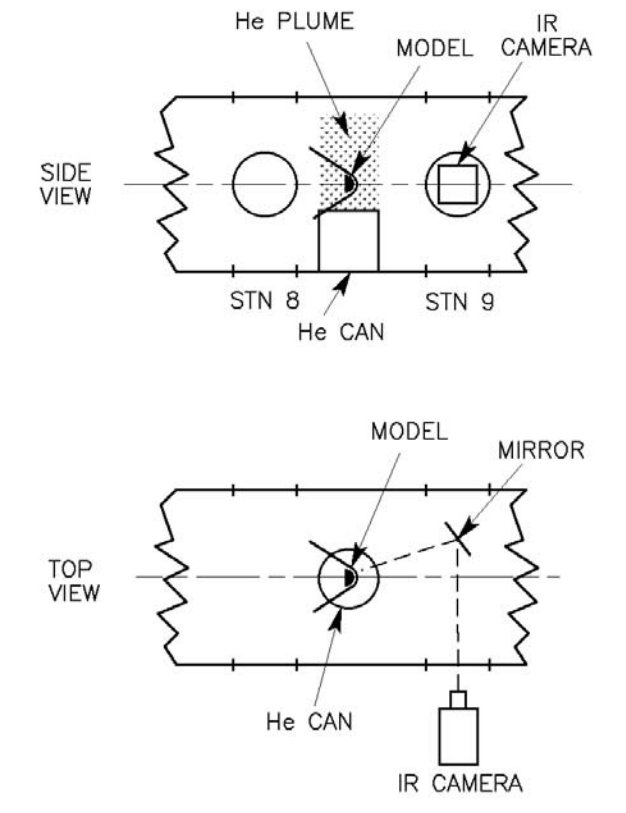

Figure 2. Representative set-up for the infra-red (IR) cameras. Model flies from left to right. A helium plume is used to strip the glowing gas cap from the model so that the camera can measure only the emission from the model surface without confounding radiation from the gas cap. This allows the model surface temperatures and, hence, heat transfer rates to be determined.

III. PERFORMANCE OF PUSHER PLATES AND OBTURATOR CUPS FOR OPEN FRONT SABOT LAUNCH PACKAGES

In this section, the performance of pusher plates and obturator (seal) cups for open-front sabot launch packages with 30 degree and 45 degree sphere-cone models is discussed. Model diameters were 3.03 and 3.30 cm and the nose radii were 0.76 and 0.114 cm. The models had differing roughnesses on the nose and the conical skirt or had a roughness band just aft of the

sphere-cone tangency point. The object of the tests discussed in this paper was to study heating augmentation due to transition and roughness-augmented heat transfer. Model velocities were 2.9 to 3.5 km/sec and range pressures were 76 to 304 Torr. Further details of the shots, models, sabots and obturators (seals) are given in Table 1 below.

Table 1. Shot conditions, model, sabot and obturator configurations for sphere-cone shots with open front sabots.

Shot number	Model cone angle (deg)	Model roughness	Sabot material	Obturator type	Obturator material	Range pressure (Torr)	Mid-range velocity (km/sec)
2677	30	Rough band	ST-801	Pusher plate	ST-801	304	3.38
2678	30	Rough band	ST-801	Pusher plate	ST-801	215	3.42
2679	30	Rough band	ST-801	Cup REV A	ST-801	304	3.40
2680	30	Rough band	ST-801	Cup REV A	ST-801	228	3.44
2681	30	Rough band	ST-801	Pusher plate	ST-801	241	3.40
2682	30	Rough band	ST-801	None	---	181	3.46
2683	30	Rough nose	ST-801	Cup REV A	UHMW PE	228	3.48
2684	30	All rough	ST-801	Cup REV B	UHMW PE	228	3.48
2685	30	All rough	ST-801	Cup REV A	UHMW PE	228	3.47
2686	30	All rough	ST-801	Cup REV C	UHMW PE	228	3.41
2687	30	All rough	ABS	Cup REV C	UHMW PE	228	3.35
2688	30	Rough band	ABS	Cup REV C	UHMW PE	202	3.37
2689	30	All rough	ST-801	Cup REV C	UHMW PE	228	3.45
2693	45	Rough nose	ST-801	Cup REV C	UHMW PE	76	3.48
2697	45	All rough	ST-801	Cup REV D	UHMW PE	114	2.95
2698	45	All rough	ST-801	Cup REV D	UHMW PE	114	2.92
2699	45	All rough	ST-801	Cup REV D	UHMW PE	114	2.93
2701	45	All rough	ST-801	Cup REV D	UHMW PE	114	2.91

Notes: 30 deg cone angle models are of 304 stainless steel and have a diameter of 3.03 cm
45 deg cone angle models are of Ti-6Al-4V titanium alloy and have a diameter of 3.30 cm
Model nose radii are 0.76 cm except for shot 2688, with a nose radius of 0.114 cm
ST-801 denotes super tough ST-801 Nylon, ABS denotes acrylonitrile-butadiene-styrene
UHMW PE denotes ultra high molecular weight polyethylene
Roughness bands start at sphere-cone tangency point

Figure 3 shows a photo of a representative launch package, with a section drawing shown in Fig. 4. Figure 5 shows the pusher plate and the 4 types of obturator (seal) cups (REV A to REV D) tested. Figure 6 shows the corresponding mid-wave (3 – 5 microns) infra-red photos taken mid-way down the range. While there is some variation in the nose roughness amongst these five images, the effect of the obturator cup can be seen on the aft part of the cone of the model. Figure 7 shows a discarded REV C obturator cup flying down the range aft of the model.

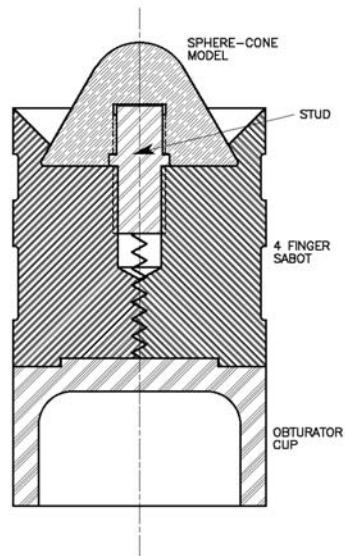
Fig. 3. Photo of launch package for open front sabot.

Fig. 4. Section drawing of launch package for open front sabots. Shown with revision A (REV A) obturator cup.
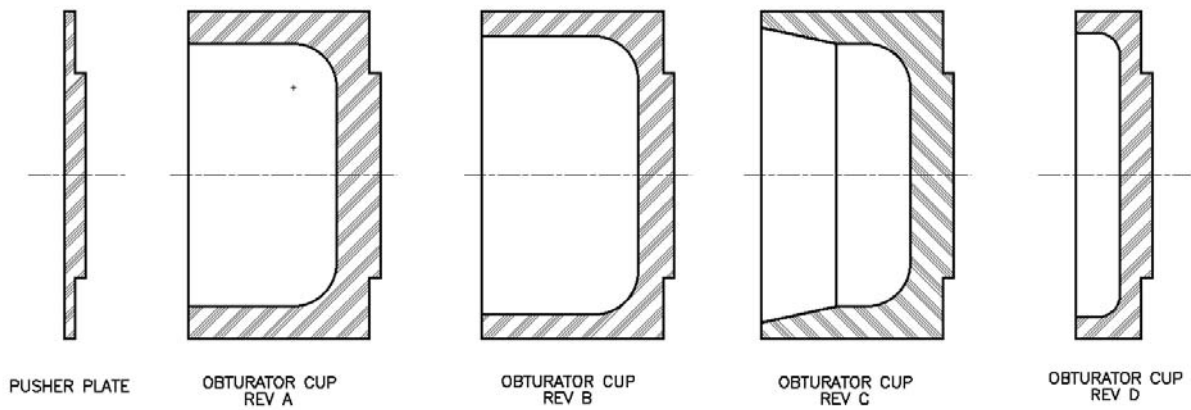
Fig. 5. Pusher plate and obturator cups for open front sabots.

(a) shot 2681   (b) shot 2685   (c) shot 2684

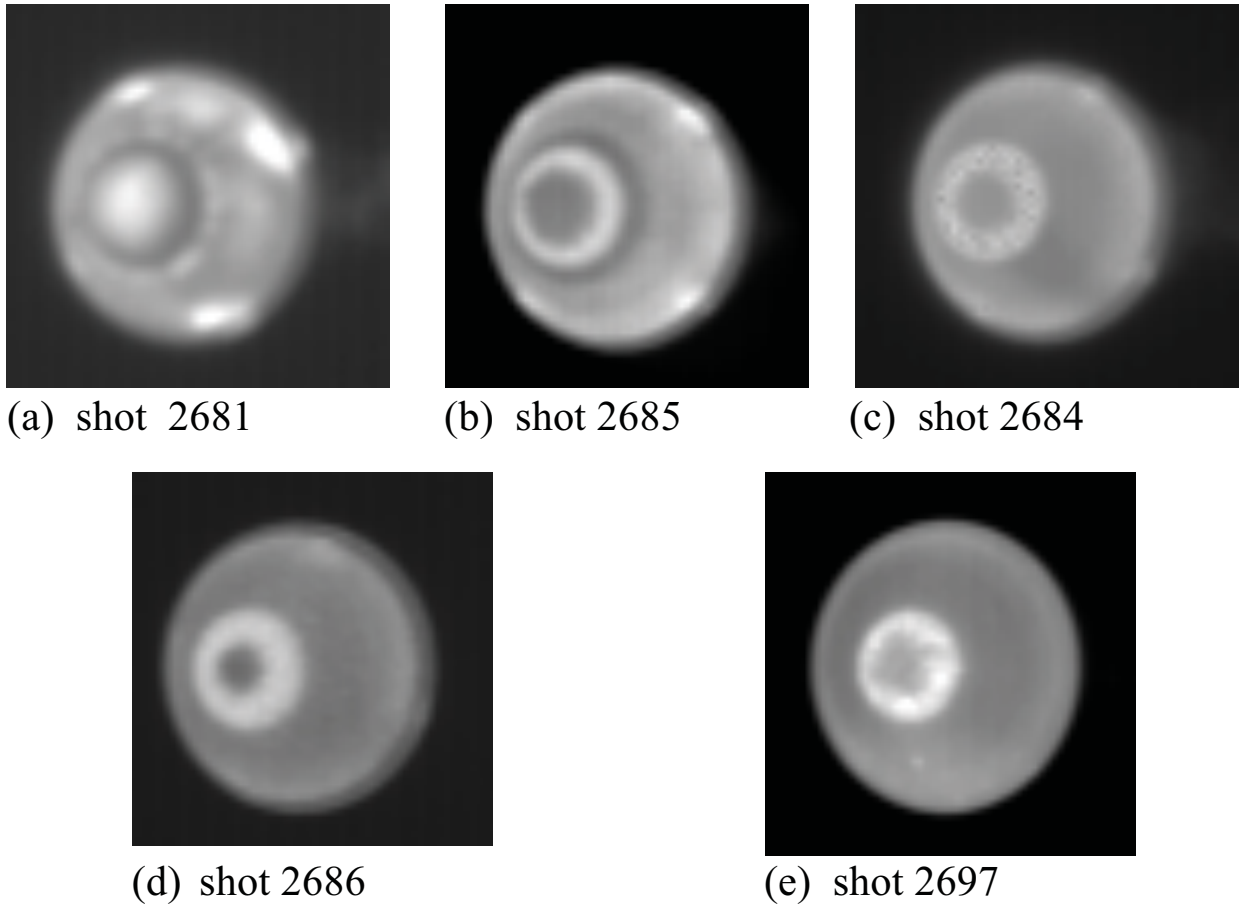(d) shot 2686   (e) shot 2697

Fig. 6. Infra-red (3 – 5 micron wavelength range) photos of sphere-cone models taken at station 8, midway down ballistic range. (a) with pusher plate, (b) – (e), with obturator cups REVs A through D, respectively. The model nose radius is 0.76 cm, velocities are 3.0 – 3.5 km/sec, range pressures are 114 – 241 Torr. Models (a) through (d) are 304 stainless steel with a 30^0 cone angle and a diameter of 3.03 cm; model (e) is Ti-6Al-4V titanium alloy with a 45^0 cone angle and a diameter of 3.30 cm. The thermal hot spots on the aft part of the model cone are indicative of the obturator cup effectiveness.
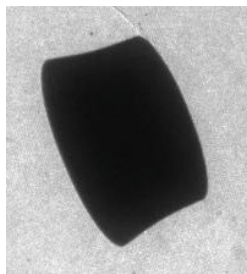

Fig. 7. Discarded REV C obturator cup flying down range aft of model.

When the pusher plate is used, a relatively poor seal is made between the drive gas and the sabot fingers and it is believed that the drive gas leaks along the grip lines of the serrations between the sabot fingers and produces a bright thermal imprint on the model seen in Fig. 6a. To try to alleviate this problem, the REV A obturator cup was instituted. The first two REV A obturator cups were made of ST-801 Nylon and disintegrated upon launch. The obturator cup

material was then switched to ultra-high molecular weight polyethylene and the cup remained intact down the range. The thermal imprints were substantially reduced, but some imprinting still remained (see Fig. 6(b)). A thinner wall obturator cup (REV B) was then tried, which ideally should have provided a better seal, since the thinner cup walls would be driven out harder against the tube wall by the pressure of the drive gas. This produced a further reduction in the thermal imprint (see Fig. 6(c)), but the cup flattened out almost completely after leaving the muzzle and then recovered its shape. Also, a piece of the obturator cup broke off. This led to a tapered wall obturator cup design (REV C). With this obturator cup design, there is almost no evidence of thermal imprints (see Fig. 6(d)). This design was used very successfully for a number of shots. In the sabot separation videos and shadowgraphs, it was noted that this obturator cup design ends up with the rear flared out by ~12 degrees (see Fig. 7), but still maintains its overall integrity.

With a 30 degree cone stainless steel model and ~210 Torr pressure in the range, the REV C obturator cup was successfully discarded. (That is, the obturator cup rapidly fell behind the model after the launch package exited the gun muzzle.) With a 45 degree titanium model and ~76 Torr pressure in the range, the REV C obturator cup drafted behind the model, caught up with and impacted the model (see Fig. 8). Hence, the reduced mass REV D obturator cup was designed (with a mass of 4.7 g versus 10.9 g for the REV C cup). The REV D obturator cup has been used successfully for a number of shots. There is no evidence of thermal imprints with this obturator design (see Fig. 6(e)).
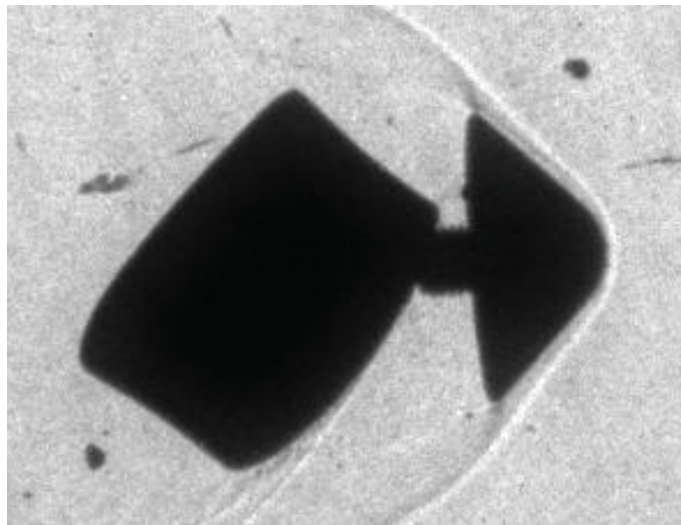

Fig. 8. REV C obturator cup impacting model.

IV. PERFORMANCE OF SABOTS AND OBTURATOR CUPS FOR
ENCLOSED SABOT LAUNCH PACKAGES

One approach to dealing with the unknown in-barrel heating, which complicates heat flux measurements in the ballistic range, is to eliminate it by enclosing the model within the sabot. To avoid sabot material transfer to the model, which could change the model's thermal response in free flight, the sabot must remain set away from the model forebody surface when the launch package is in the gun barrel. In this section, the performance of enclosed sabots and the

corresponding obturator cups for launch packages with 45 degree sphere-cone models is discussed. Model diameters were 3.30 cm and the nose radii were 0.76 cm. The models had differing roughnesses on the nose and conical skirt. Model velocities were 2.5 to 2.6 km/s and range pressures were 76 Torr. Further details of the shots, models, sabots and obturators are given in Table 2 below.

Table 2. Shot conditions, model, sabot and obturator configurations for sphere-cone shots with enclosed sabots.

Shot number	Model cone angle (deg)	Model roughness	Sabot material	Obturator type	Obturator material	Range pressure (Torr)	Mid-range velocity (km/sec)
2691	45	All smooth	ST-801	Cup REV E	UHMW PE	76	2.53
2692	45	All rough	ST-801	Cup REV F	UHMW PE	76	2.55
2694	45	All rough	ST-801	Cup REV G	UHMW PE	76	2.57
2695	45	All rough	ST-801	Cup REV H	UHMW PE	76	2.53
2696	45	All rough	ST-801	Cup REV H	UHMW PE	76	2.58

Notes: Models are of Ti-6Al-4V titanium alloy and have a diameter of 3.30 cm
       Model nose radii are 0.76 cm
       ST-801 denotes super tough ST-801 Nylon
       UHMW PE denotes ultra high molecular weight polyethylene

Figure 9 shows photos of launch packages with revision E (REV E) and H (REV H) obturator cups. Figure 10 shows sectional drawings of the same two launch packages. Figure 11 shows the 4 types of obturator cups (REV E to REV H) tested. Figure 12 shows the corresponding mid-wave (3 – 5 microns) infra-red photos taken mid-way down the range.
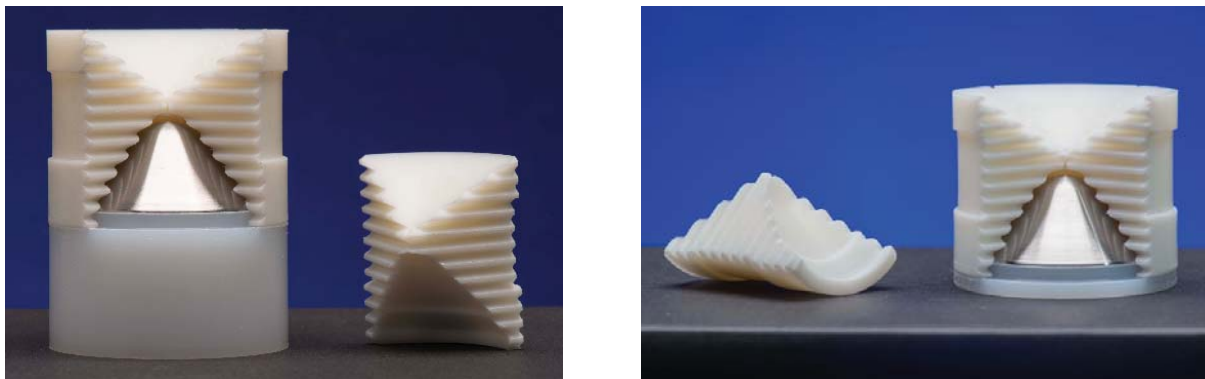

Fig. 9. Photos of two launch packages for enclosed sabots. Shown with revision E (REV E) (left photo) and H (REV H) (right photo) obturator cups.
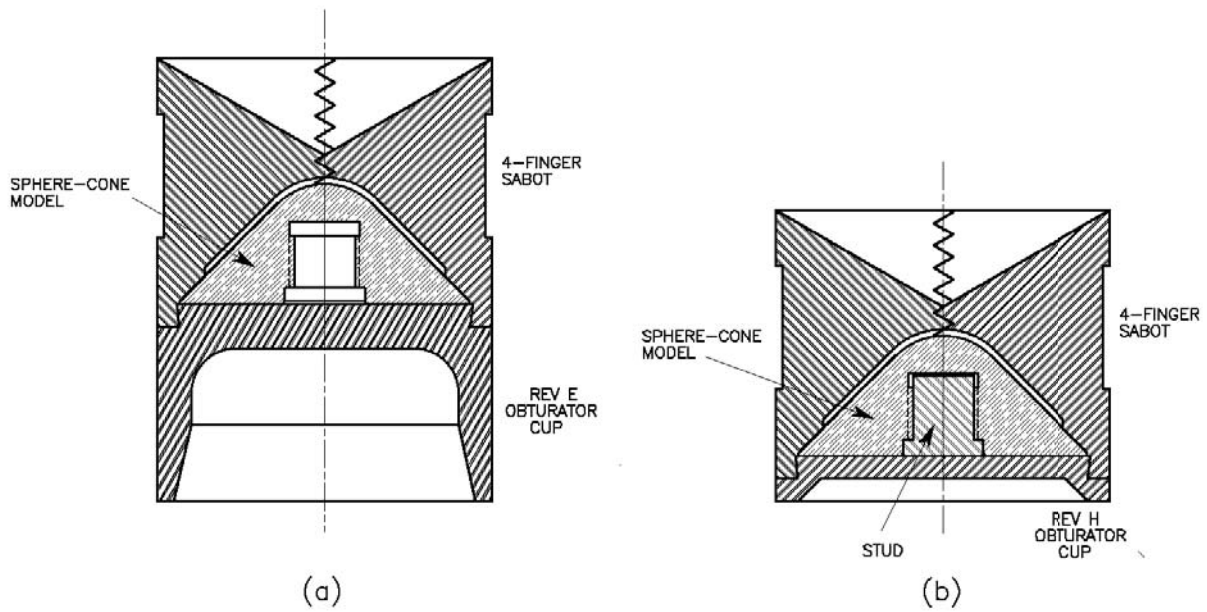
Fig. 10. Section drawings of two launch packages for enclosed sabots. Shown with (a) revision E (REV E) and (b) with revision H (REV H) obturator cups. Left package has no stud in the model while the right package drawing shows the stud in the model used for the second of the two shots made with the REV H obturator cups.
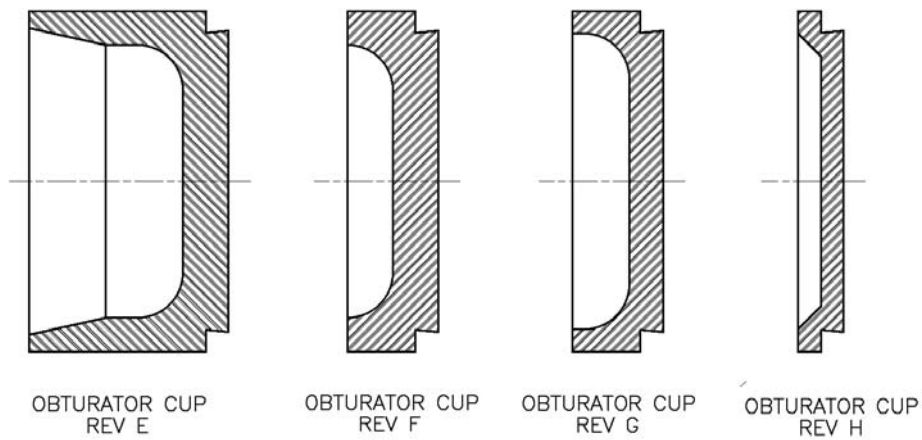

Fig. 11. Obturator cups for enclosed sabots. Masses of obturator cups are (in order) 10.9, 7.3, 6.4 and 3.0 g.
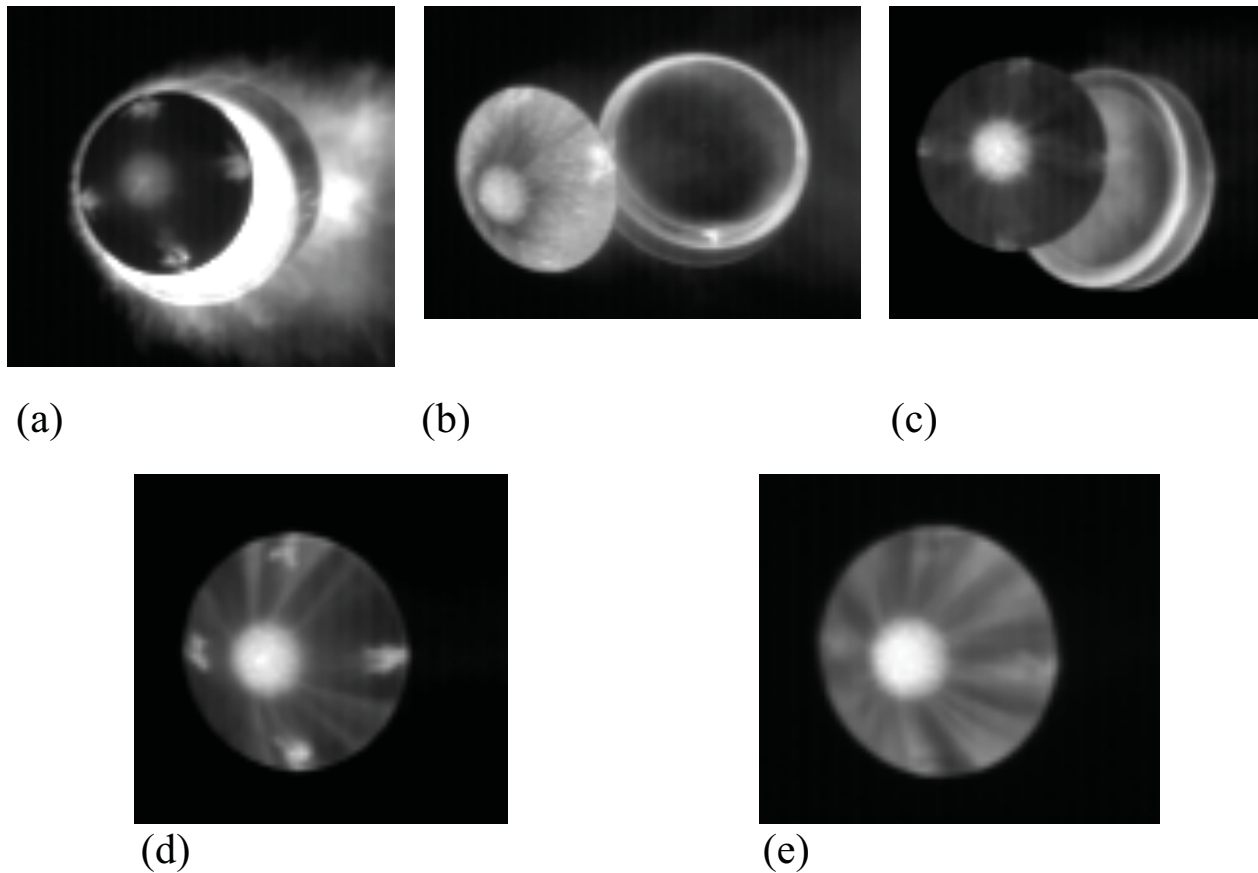
Fig. 12. Infra-red (3 – 5 micron wavelength range) photos of sphere-cone models taken at station 8, midway down ballistic range. (a) – (e) with obturator cups REVs E, F, G, H and H, respectively. (Shots 2691, 2692, 2694, 2695 and 2696, respectively.) The model nose radius is 0.76 cm, velocities are 2.5 – 2.6 km/sec, range pressures are 76 Torr. Models are Ti-6Al-4V titanium alloy with a 45^0 cone angle and a diameter of 3.30 cm. Note that obturator discs can be seen close behind models in photos (a) – (c).

With the heavy (10.9 g) REV E obturator cup, the cup drafted strongly, remained close behind the model [(see Fig. 12(a)], impacted the model several times between shadowgraph stations 1 and 13 and only started to fall behind the model at shadowgraph station 14. The impacts caused large pitch and yaw angle oscillations of the model. With the lighter (6.4 – 7.3 g) REV F and REV G obturator cups, the cups still drafted significantly, remained relatively close behind the model [see Figs. 12(b) and 12(c)], impacted the model at least once between shadowgraph stations 1 and 3 and started to fall behind the model at shadowgraph station 4. The obturator cups were 2 to 4 cm behind the model at shadowgraph station 8. Large model pitch and yaw angle oscillations were also seen with these two shots. With the still lighter (3.0 g) REV H obturator cups, the obturator cup is discarded successfully and does not appear in any shadowgraphs (although in the full frame photo from which Fig. 12(e) is cropped, it can be seen well behind the model). Model pitch and yaw angles are small – the largest angles are typically ~5 degrees.

With the first shot with the REV H obturator cup, the stud shown within the model in Fig. 10 was not used and the gas pressure in the launch tube caused the thin obturator cup to extrude into the hole in the model. (The hole in the model is necessary for machining and bead blasting operations.) The extruded obturator cup material can be seen in the sabot separation photo in Fig. 13(a). For the next shot, this problem was eliminated by installing the stud in the model. For this shot, no extrusion of obturator cup material is seen in the sabot separation photo [see Fig. 13(b)].
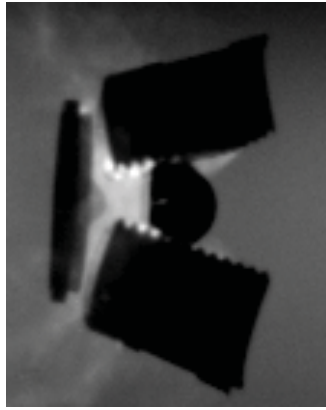
(a)   (b)

Fig. 13. Sabot separation photos for launch packages with REV H obturator cups. (a) without stud shown in Fig. 8(b) in model; (b) with stud in model. Models are flying from left to right.

In Fig. 12, four-fold symmetric "imprints" are seen on the models. They are brightest for Figs. 12(a), (b) and (d) and much fainter in Fig. 12(c). Very faint "imprints" may possibly be seen in Fig. 12(e), but are hard to distinguish from the streaks, which may be due to incomplete transition to turbulence. These "imprints" bear some resemblance to those seen in Figs. 6(a) and (b) for the 30 degree cone open sabot launches, but their shapes are somewhat different. We currently believe that these "imprints" for the enclosed sabots are not caused by the drive gas in the barrel leaking past the obturator and through the serration joints to reach to model forebody, as was the case for the open front sabot launch packages. Rather, it is believed that, after the launch package exits the gun muzzle, and the shock heated ambient gas forms in front of the sabot fingers, the hot gas, along with the ablated Nylon sabot material, leaks back through the serration joints and, in the neighborhood of the joints, deposits some Nylon on the model. The Nylon deposits are believed to cause the "imprints" seen in Figs. 12. Figure 14(a) shows the shock heated gas cap in front of the launch package 21 cm down range from the gun muzzle for shot 2696. Figure 14(b) shows the launch package 184 cm down range from the gun muzzle for the same shot. The aerodynamically heated sabot fingers and the smoke coming off the fingers
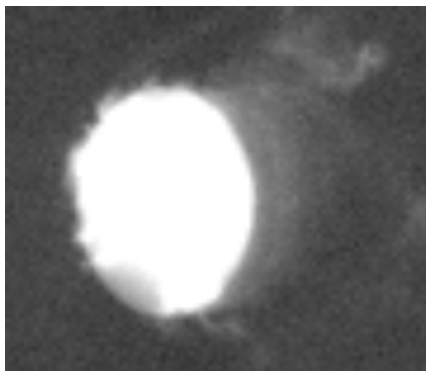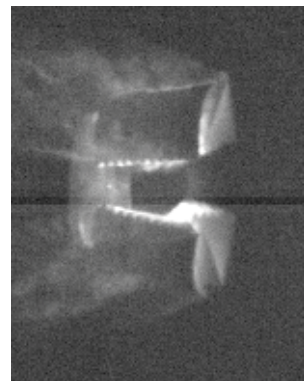
(a)   (b)

Fig. 14. (a), photo of launch package 21 cm downrange of the gun muzzle for shot 2696, (b) photo of launch package 184 cm downrange of gun muzzle for the same shot. Range pressure is 76 Torr.

are evident. For the open front sabot launch package, there is no Nylon upstream of the model except for a narrow grip zone (Figs. 3 and 4) and it is believed that deposition of Nylon on the model forebody is not a problem.

It must be noted that the explanation given above for the "imprints" seen in Fig. 12 is not definitive at the present time. However, since significant "imprints" were present in four of the five enclosed sabots shots and were absent or very nearly so for open front sabot shots with the REV C and REV D obturator cups, it was decided to go with the open front sabot design. In general, there is a second reason to favor the open front sabot design. Stress calculations indicate that the front of the enclosed sabot design (see Figs. 9 and 10) will collapse on to the model at launch velocities of 3 to 4 km/s (depending upon the sabot finger material) and above. This would be totally unacceptable, of course, because of contamination of the model and possible changes to the model roughness. On the other hand, the open front sabot design (see Figs. 3 and 4) has been successfully used at launch velocities up to 6 km/s.

V. USE OF SPECIAL GASES IN THE LAUNCH TUBE TO REDUCE IN-BARREL HEATING

Another approach to dealing with the unknown in-barrel heating is to greatly reduce that heating by using special gases in the launch tube. One may use the same gas that is being used in the range at a greatly reduced pressure or one may use a light gas such as helium or hydrogen, still at a somewhat lower pressure than that in the range. The heat transfer reductions can be assessed using the following equations. From Ref. 6, with slight modifications, we have

$$q_w = hA_w(T_w - T) \hspace{3cm} \text{Eq. (1)}$$

where:

q_w = wall heat flow
h = heat transfer coefficient
A_w = wall area
T_w = wall temperature
T = gas total temperature

The Stanton number (St) is defined in Ref. 6 as

$$St = \frac{h}{\rho C_p u} \hspace{3cm} \text{Eq. (2)}$$

where:

C_p = specific heat at constant pressure of barrel gas
u = velocity
ρ = density

For a turbulent boundary layer with Reynolds numbers (Re) between 5 x 10^5 and 10^7, Ref. 7 gives an expression of the following form for St

$$St\, Pr^{2/3} = 0.0296\, Re^{-0.2} \hspace{3cm} \text{Eq. (3)}$$

where:

$$\text{Pr} = \frac{\mu C_p}{k}$$

$$\text{Re} = \frac{\rho u x}{\mu}$$

μ = viscosity
k = thermal conductivity
x = distance from start of boundary layer

Combining Eqs. (1) – (3), we get

$$F = \frac{q_w}{A_w} = \rho C_p u (T_w - T) 0.0296 \, \text{Re}^{-0.2} \, \text{Pr}^{-2/3} \qquad \text{Eq. (4)}$$

For a given gun launch condition, but considering two different gases (in this case air and hydrogen) in the launch tube, we have very nearly equal values of $C_p(T - T_w) = u^2/2$, which is the enthalpy difference due to motion at velocity u. (The difference in velocity caused by the gas in the barrel is typically only a few per cent.) Furthermore, the Prandtl numbers of air and of hydrogen are very nearly equal.[8] Hence, we can write

$$F \propto \rho \left(\frac{1}{\text{Re}} \right)^{0.2} \propto \rho \left(\frac{\mu}{\rho u x} \right)^{0.2} \qquad \text{Eq. (5)}$$

For the same gun size and muzzle velocity

$$F \propto \rho^{0.8} \mu^{0.2} \qquad \text{Eq. (6)}$$

From Eq. (6), for 2 Torr air in the launch tube and 95 Torr air in the range, we have

$$F_{\text{special gas}}/F_{\text{open barrel}} = 0.046$$

In this case, the "special gas" is air at a lower pressure than in the range. For 43 Torr hydrogen in the launch tube and 95 Torr air in the range, we have

$$F_{\text{special gas}}/F_{\text{open barrel}} = 0.054$$

To make the latter calculation, we have used the viscosities of hydrogen and air from Ref. 9. Thus, by greatly reducing the gas pressure in the launch tube or by using hydrogen in the launch tube at a somewhat reduced pressure, the in-barrel heating should be able to be reduced to roughly 5% of that obtained when an open barrel is used.

An advantage of using hydrogen in the launch tube instead of the range gas (which usually is air) is that the hydrogen will be less compressed by the oncoming launch package than the air would be and hence there will a longer slug of gas in front of the launch package when hydrogen is used. This would allow more time for the diaphragm fragments to clear the model path in front of the muzzle when hydrogen is used. This, of course, is necessary so that the diaphragm fragments do not impact the front of the model. (This problem will be discussed further below.) Estimates of the compression of air versus that of hydrogen, either by a shock wave, or by many continuous waves, indicate that the slug of hydrogen in front of the launch package will be on the order of twice the length of the corresponding slug of air. Effective clearing away of the

diaphragm fragments from the model path in front of the muzzle will require not only a substantial length of the compressed gas slug from the launch tube, but also, a sufficient density of gas. For example, a very low pressure of hydrogen in the launch tube may not be able to effectively clear the diaphragm fragments.

Table 3 gives the shot conditions and launch tube gases for all shots with special gases in the launch tube. In earlier test entries, 0.0025 cm thick clear Mylar muzzle diaphragms were used.

Table 3. Shot conditions and launch tube gases.

Shot number	Mid-range velocity, v (km/sec)	Range pressure (Torr)	Barrel gas	Barrel gas pressure (Torr)	T(package exit) - T(dia break) = ΔT (microsec)	v x ΔT pressure (cm)	Notes
2691	2.53	76	Air	<1	Break not visible	---	See #1
2692	2.55	76	Air	0.5	Break not visible	---	
2694	2.57	76	Air	0.7	Break not visible	---	
2695	2.53	76	Air	1.5	123	31	
2696	2.58	76	Air	1.5	288	74	See #2
2697	2.95	114	Hydrogen	3	41	12	
2698	2.92	114	Air	3	178	52	See #3
2699	2.93	114	Hydrogen	29.2	178	52	
2701	2.91	114	Hydrogen	43.2	411	120	
2702	2.72	76	Hydrogen	42.2	274	75	
2703	2.93	114	Hydrogen	42.6	397	116	

Notes: #1: diaphragm fragments visible in front of model in sabot separation video
    #2: diaphragm fragment visible to side on model path in muzzle video
    #3: diaphragm fragments visible in several muzzle video frames; impact of diaphragm fragment on model visible in muzzle video frame; impact damage to model forebody visible in mid-range infrared photo

The clear Mylar was very difficult to see in the muzzle videos. For the present test series, for shots 2694 and later, 0.0025 cm thick aluminized Mylar was used, which was much easier to see in the videos. With the back lighting by the glowing gas in the launch tube, there is a fairly good contrast between the now opaque diaphragm fragments and the open spaces between the fragments.

For shot 2691, with air at a pressure of <1 Torr in the launch tube, the sabot separation video frame shown in Fig. 15(a), taken 1.03 m from the muzzle, shows diaphragm fragments in front of the launch package. For shot 2696, with air at a pressure of 1.5 Torr in the launch tube, the muzzle video frame shown in Fig. 15(b) shows a diaphragm fragment off to the side of the launch package, just exiting the muzzle. (The fragment is actually out of the path of the launch package, but appears to be directly in front of the launch package in the photo because of the tilt of the viewing angle.) For shot 2698, with air at a pressure of 3 Torr in the launch tube, the muzzle video frame shown in Fig. 16(a), taken 137 microsec before launch package exit, shows diaphragm fragments in the path of the launch package. The frame shown in Fig. 16(b) taken 41 microsec after launch package exit, shows a diaphragm fragment impacting the model. An infra-red photo for this shot [Fig. 16(c)], taken mid-way down the range, shows the damage to the model caused by the impact of the diaphragm fragment.

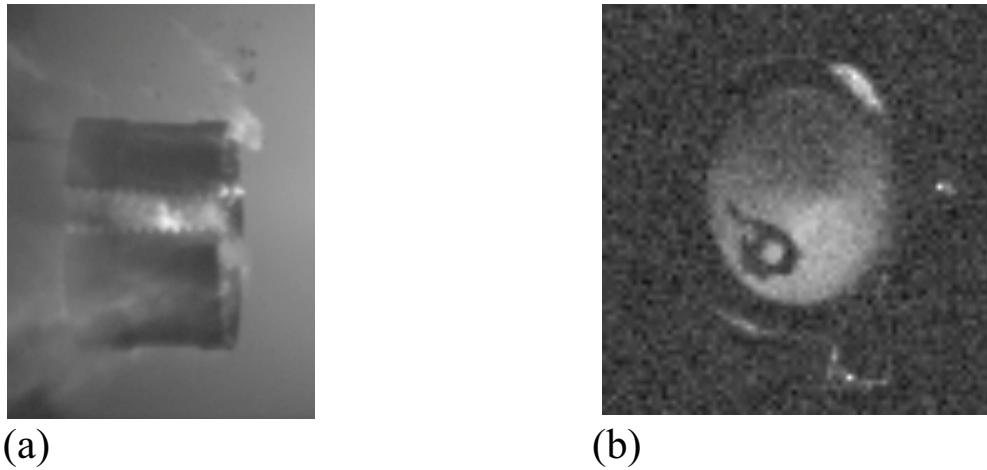(a)   (b)

Fig. 15. (a), shot 2691, sabot separation frame taken 1.03 m from the muzzle, (b) shot 2696 muzzle video frame taken just as launch package exits muzzle. Range pressures are 76 Torr and mid range model velocities are 2.53 km/sec.

(a)   (b)   (c)
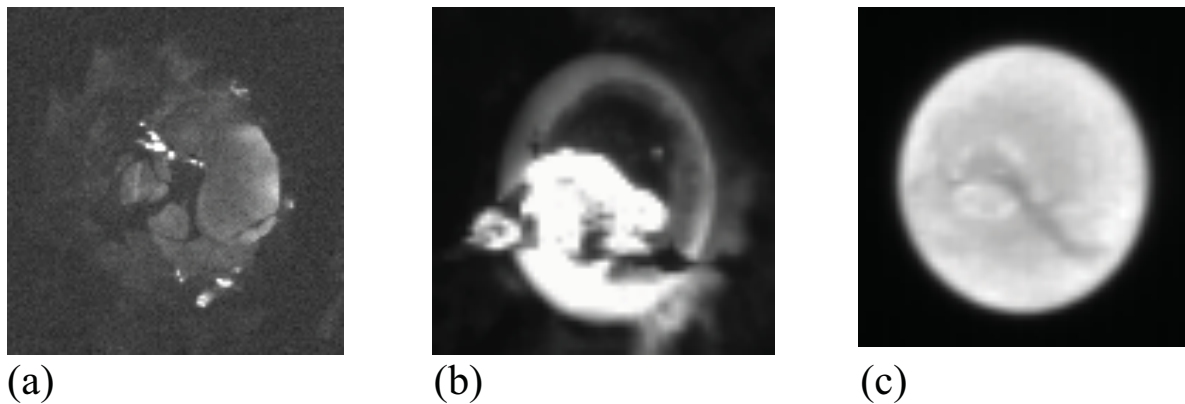
Fig. 16. (a), shot 2698, muzzle video frame taken 137 microsec before launch package exit, (b) muzzle video frame taken 41 microsec after launch package exit, (c), infra-red photo taken mid-way down the range. Range pressure is 114 Torr and mid range model velocity is 2.92 km/sec.

For shot 2699, with hydrogen at a pressure of 29 Torr in the launch tube, the muzzle video frames shown in Fig. 17, taken 41 and 55 microsec after launch package exit, show what appear to be light strikes against the model, which could be caused by small diaphragm fragments.

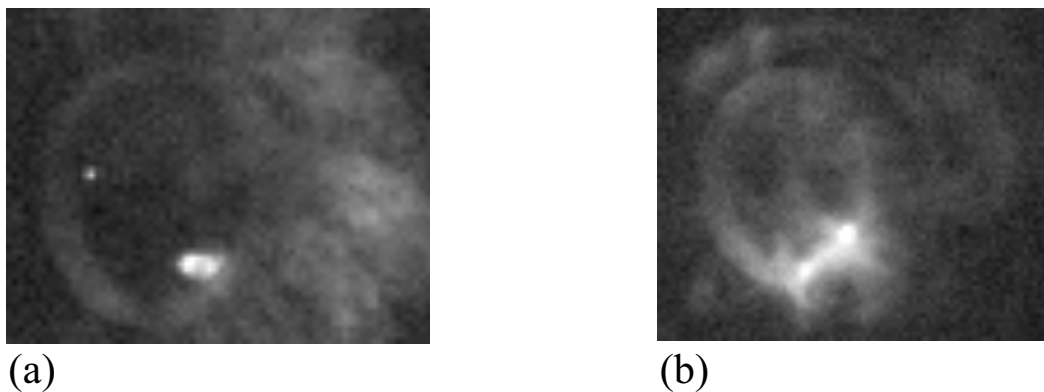(a)   (b)

Fig. 17. Shot 2699, muzzle video frames taken (a) 41 microsec and (b) 55 microsec after launch package exits muzzle. Range pressure is 114 Torr and mid range model velocity is 2.93 km/sec.

Figure 18 shows the infra-red photos taken midway down the range for shots 2698, 2699 and 2701 – 2703. [Figure 18(a) is a repeat of Fig. 16(c).] There is no damage seen in Fig. 18(b) which corresponds to the light strikes that are seen in Fig. 17. Light strikes were also seen in the muzzle video frames for shot 2702, but not for shots 2701 and 2703. Irregularities seen in the central dark zone in Figs. 18 (b), (c) and (e), as well as the streaks seen on the cone in Fig. 18(d) are believed to be due to non-uniform transition and not to damage to the model. The configuration with 29 to 43 Torr of hydrogen in the launch tube, producing the high quality infra-red photos seen in Figs. 18, (b) through (e), appears to be very satisfactory. This configuration should, as discussed earlier, be able to reduce the in-barrel heating to about 5% of the value obtained with the open barrel, thus greatly reducing the uncertainty in the range heat flux measurements due to unknown in-barrel heating.

(a)   (b)   (c)
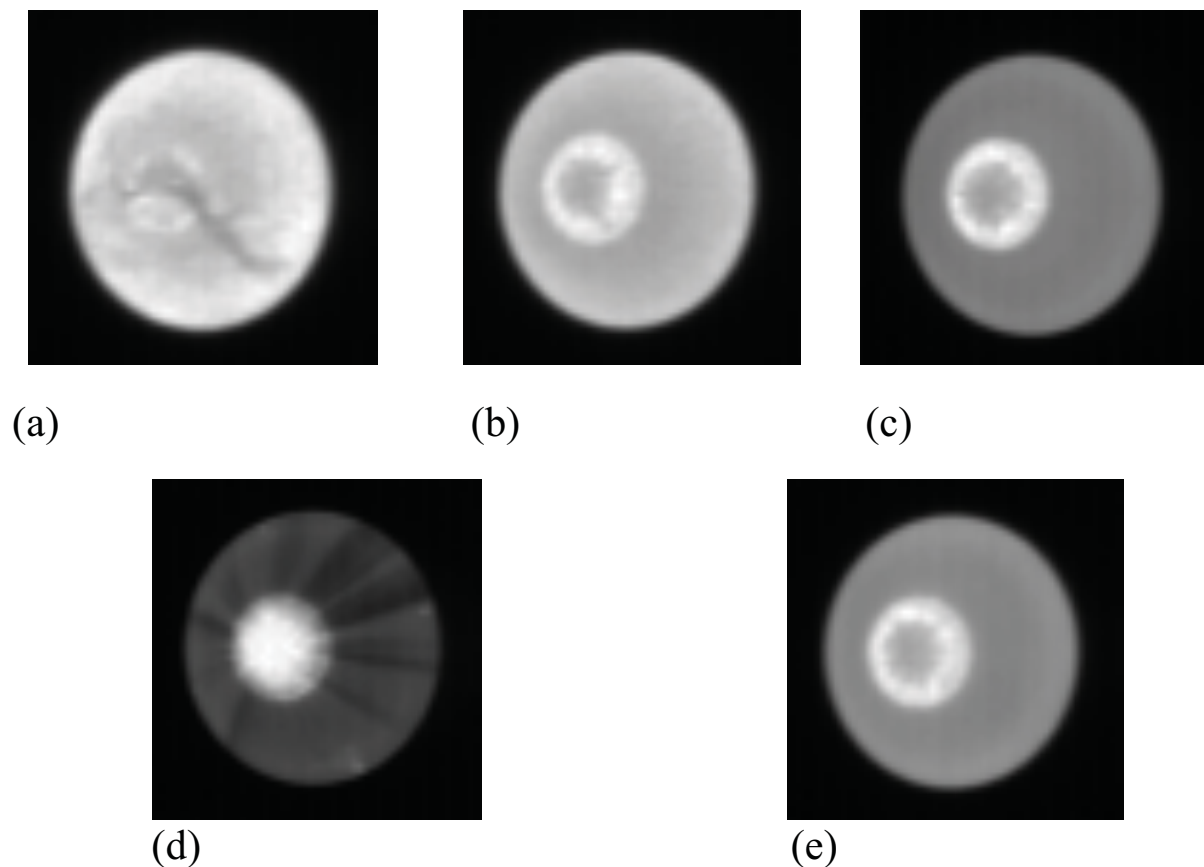
(d)   (e)

Fig. 18. Infra-red (3 – 5 micron wavelength range) photos of sphere-cone models taken at station 8, midway down ballistic range. (a), shot 2698, (b), shot 2699, (c), shot 2701, (d), shot 2702 and (e), shot 2703. Velocities are 2.72 – 2.93 km/sec, range pressures are 76 - 114 Torr.

Column 6 of Table 3 gives the time between diaphragm rupture and exit of the launch package at the gun muzzle. Multiplying this delta time by the model velocity gives an estimate of the length of the compressed gas slug in front of the model in the launch tube at diaphragm rupture (shown in column 7 of Table 3). There is some correspondence between these experimental lengths and what would be expected theoretically, but the correspondence is not perfect. For shots 2701 – 2703, with ~43 Torr of hydrogen in the launch tube, relatively large slug lengths of 75 – 120 cm were obtained. For shots 2695 and 2698, with 1.5 – 3.0 Torr of air in the launch tube, slug lengths of 31 – 52 cm were obtained. This is as expected, following the

earlier discussion in this section of air versus hydrogen in the launch tube. For shot 2697 with 3.0 Torr of hydrogen in the launch tube, a very short slug length of 12 cm was obtained. One might have expected a long slug length for this case (as for shots 2701 – 2703) but, with a very low hydrogen pressure in the launch tube, the hydrogen must be much more highly compressed to break the diaphragm, which could explain the short slug length. However, for shot 2696 with 1.5 Torr of air in the launch tube, a rather long slug length of 74 cm was obtained. Also, for shot 2699, with 29 Torr of hydrogen in the launch tube, a slug length of 52 cm was obtained. This is significantly shorter than the slug lengths with ~43 Torr of hydrogen in the launch tube and is equal to the slug length with 3 Torr of air in the launch tube. For these last two shots, the experimentally estimated slug lengths do not line up with those expected theoretically. At the present time, we do not have explanations for these disagreements.

As discussed above, for mid-range velocities of 2.7 – 3.0 km/sec, range pressures of 76 – 114 Torr and hydrogen pressures of 29 – 43 Torr in the launch tube, the hydrogen-in-barrel technique worked very well. However, for a later shot with a mid-range velocity of 5.1 km/s, a range pressure of 50 Torr and 42 Torr of hydrogen in the launch tube, the technique failed to clear the diaphragm fragments from the model path and the model impacted the fragments, damaging the model. At the higher velocity, the hydrogen is compressed more strongly, leading to a shorter slug of hydrogen in the barrel in front of the model. Also, there is substantially less time for the diaphragm fragments to clear the model path. Possible fixes for using the hydrogen-in-barrel technique at higher velocities are (1) raise the hydrogen pressure from 42 Torr to 84 Torr, (2) switch from 0.0025 cm thick Mylar diaphragms to 0.0013 cm thick Mylar diaphragms, (3) use helium (which is less compressible then hydrogen) instead of hydrogen as the barrel fill gas and (4) combinations of (1), (2) and (3). At present, the effectiveness of these fixes has not yet been demonstrated.

VI. SUMMARY AND CONCLUSIONS

For the design of thermal protection systems (heat shields) for entry of space vehicles into atmospheres of the earth or other planets, it is important to be able to predict the heat transfer to the vehicles during atmospheric entry. Vehicle surface roughness can cause augmentation of the heat transfer up to values of the order of 70%. In the NASA Ames HFFAF ballistic range, a systematic study of roughness-augmented heat transfer has been undertaken. The heat transfer was measured by using infra-red cameras to measure the model temperature variations down the range, from which the heat transfer rates can be calculated. Several different phenomena can, however, confound these measurements. First, the hot drive gas in the gun barrel behind the launch package can leak through the sabot (model carrier) joints and create confounding thermal imprints on the model forebody. Second, when the sabot fingers extend in front of the model, hot sabot material can flow backwards and deposit on the model forebody, changing its thermal characteristics. Third, with open front sabot designs, an unknown amount of heating of the model forebody can occur in the launch tube.

The first of these problems was addressed by providing a cup-shaped obturator behind the sabot fingers (which separate after the launch package exits the gun muzzle) to try to prevent any of the hot drive gasses from reaching the model forebody. Several obturator cup designs for open front sabots were discussed; the last design worked very well in blocking the gun drive gas. Some of the earlier, heavier obturator cups drafted behind the model and then impacted the model; the last design was much lighter and avoided this problem.

One way of dealing with unknown in-barrel heating is to enclose the model within the sabot. Several such designs, with different obturator cups, were tested. The earlier, heavier, obturator cups, again, drafted behind the model and then impacted the model; the last, lightest obturator cup avoided this problem. In general, "imprints", which may be due to deposition of sabot

material, were seen on the model forebody using this technique; hence, it was abandoned in favor of the open front sabot design.

Another way of dealing with unknown in-barrel heating is to greatly reduce the pressure of the test gas in the barrel or to replace the test gas (usually air) in the barrel with hydrogen, at a somewhat reduced pressure. Air at 0.5 – 3 Torr pressure (cf. test gas pressure of 76 – 114 Torr.) did not work well; diaphragm fragments frequently did not clear the model path. For mid-range velocities of 2.7 – 3.0 km/s, hydrogen at 43 Torr pressure was found to work very well, clearing the diaphragm fragments away from the model path. The same technique did not successfully clear the diaphragm fragments from the model path at a mid-range velocity of 5.1 km/s. Fixes for the problem at the higher velocities were suggested, but not yet demonstrated.

In summary, the best combination of techniques was (1) the open front sabot design with a light, but well-sealing obturator disc, which sealed off the hot barrel drive gas and quickly dropped behind the model without impacting it and (2), for mid-range velocities of 2.7 – 3.0 km/s, the use of hydrogen at 43 Torr in the barrel, which greatly reduced in-barrel heating and successfully blew the diaphragm fragments out of the model path. For mid-range velocities of 5.1 km/sec, the hydrogen-in-barrel technique was not yet successfully demonstrated.

ACKNOWLEDGEMENTS

REFERENCES

1. National Research Council Committee on the Planetary Science Decadal Survey, "Vision and Voyages for Planertary Science in the Decade 2013 – 2022," The National Academies Press, Washington, D.C., 2011.
2. Beebe, R. and Dudzinski, L., "Saturn Atmosphere Entry Probe Mission Study," Planetary Science Decadal Survey Mission Concept Study Final Report, NASA, April 2010.
3. Beebe, R. and Dudzinski, L., "Saturn Atmosphere Entry Probe Trade Study," Planetary Science Decadal Survey Mission Concept Study Final Report, NASA, September 2010.
4. Hubbard, W. B., "Ice Giants Decadal Study," Planetary Science Decadal Survey Mission Concept Study Final Report, NASA SDO-12345, June 2010.
5. Wilder, M. C., Reda, D. C. and Prabhu, D. K., "Heat-Transfer Measurements on Hemispheres in Hypersonic Flight Through Air and CO_2," AIAA paper 2011-3476, 42nd AIAA Thermophysics Conference, 27 – 30 June 2011, Honolulu, Hawaii.
6. W. Holman, J. P., "Heat Transfer", 6th ed., McGraw-Hill, New York, 1986, p. 252.
7. ibid, p. 255.
8. ibid, pp. 643, 644.
9. Golubev, I. F., "Viscosity of Gases and Gas Mixtures," Israel Program for Scientific Translations, Jerusalem, 1970, p. 62.